

Short communication

## Characterization of Ni porous electrode covered by a thin film of $\text{LiMg}_{0.05}\text{Co}_{0.95}\text{O}_2$

E. Simonetti\*, R. Lo Presti

ENEA, CR Casaccia, Via Anguillarese 301, 00060 S.M. di Galeria, Rome, Italy

Available online 12 June 2006

### Abstract

A porous electrode of nickel covered by a thin film of lithium cobaltite doped with magnesium ( $\text{LiMg}_{0.05}\text{Co}_{0.95}\text{O}_2$ ) was prepared in order to protect nickel cathode against dissolution into the molten carbonate. A sol impregnation technique was used to deposit gel precursors on the porous surface of the substrate; the covered substrate was submitted to thermal treatments, which produced a lithium cobaltite layer. The cathode was characterized by the following measurements: biaxial bending test, SEM/EDX analysis, which demonstrated the uniformity of the lithium cobaltite layer and the presence of cobalt homogeneously distributed over the nickel particles, electrical conductivity.

To test the cathodic performance of the material under study a cell was assembled and tested in a  $10\text{ cm} \times 10\text{ cm}$  electrodes area plant. The cell performance during the time was studied carrying out polarization curves for many hours (more than 1000 h). To determine the influence of the cathodic gas composition on the electrode performance the atmosphere was changed maintaining alternatively at a constant value the partial pressure of  $\text{CO}_2$  and  $\text{O}_2$ . In such a way the kinetic effect of the single gas was studied. By the technique of *IR* interruption the internal resistance of the cell was measured.

© 2006 Elsevier B.V. All rights reserved.

**Keywords:** MCFC;  $\text{LiMg}_{0.05}\text{Co}_{0.95}\text{O}_2$ -coated Ni cathode; Sol impregnation; Cell performance

### 1. Introduction

Molten carbonate fuel cell (MCFC) are one of the most promising devices for power generation because of their high efficiency and low emission. The state of the art of the cathodic material is the lithiated nickel oxide,  $\text{Li}_x\text{Ni}_{1-x}\text{O}$ , for which the oxygen reduction reaction rate (oxygen reduction reaction, ORR) is high. The main problem with  $\text{Li}_x\text{Ni}_{1-x}\text{O}$  derives from the fact that its rate of dissolution in molten carbonate is very high (solubility 20–50 ppm). Like consequence of such phenomenon, the cathodic nickel is dispersed and transported inside the electrolyte producing a concentration gradient under the electric field of the cell. Moreover, the  $\text{Ni}^{2+}$  ion can be reduced to Ni in the matrix producing a short circuit of the cell. The dissolution rate depends on the pressure, and in the case of pressurized MCFC, the estimated life time highly decreases. One way to solve such problem is to add to the electrolyte a ion that makes it [1,2] more basic; an other way is to develop alternative cathodic

material [3,4]. Different materials have been studied in these years: ferrites, cobaltites, manganites, doped metallic oxides, ilmenites, spinels and perovskites. The greater part of such materials is not stable in molten carbonates and/or they react with  $\gamma\text{-LiAlO}_2$  of the matrix [5]. The more promising materials are  $\text{LiFeO}_2$  and  $\text{LiCoO}_2$ . Both have a good wettability with the electrolyte and are more stable than  $\text{Li}_x\text{Ni}_{1-x}\text{O}$  in cathodic atmosphere.  $\text{LiFeO}_2$  is less expensive, but its electrical conductivity at  $650^\circ\text{C}$  is very low ( $0.05\text{ S cm}^{-1}$ ) and sensitive to gas composition even if doped with Co, Ni, Mg and other elements. Lithium cobaltite ( $\text{LiCoO}_2$ ) is a ceramic material semiconductor and is already used commercially in lithium-ion batteries; an other field of application is in the electrochromic films. Many laboratories have studied and developed cathodes in  $\text{LiCoO}_2$  [6,7]. In ENEA laboratories, within the Agreement of Program MICA-ENEA, a process [4] for the production of the cobaltite powders and the realization, by means of tape casting, of porous cathodes of  $100\text{ cm}^2$  of dimensions has been developed. The lithium cobaltite doped with magnesium electrode has been characterized outside the cell (morphology, conductivity, solubility) and with in cell tests (polarization curves, *IR* interruption). The comparison with nickel oxide has allowed to assert that lithium cobaltite doped with magnesium can, from the electrochemi-

\* Corresponding author.

E-mail addresses: [simonettie@casaccia.enea.it](mailto:simonettie@casaccia.enea.it) (E. Simonetti), [Roberto.lopresti@casaccia.enea.it](mailto:Roberto.lopresti@casaccia.enea.it) (R.L. Presti).

cal point of view, to replace the conventional cathode. On the contrary the use of lithium cobaltite is limited from its mechanical brittleness and the high cost of the raw materials but, above all, from the process of preparation of the electrode. In order to obviate to these disadvantages it has been prepared a porous nickel cathode covered with a thin layer of lithium cobaltite doped with magnesium to maintain the properties of the metallic substrate reducing nickel solubility. Lithium cobaltite thin films have been deposited by different techniques: chemical vapour deposition, sputtering and laser ablation. The complex sol–gel process (CSGP) technique was selected in order to protect the nickel cathode against dissolution because effective and less expensive.

## 2. Experimental

### 2.1. Preparation of $\text{LiMg}_{0.05}\text{Co}_{0.95}\text{O}_2$ -coated Ni cathode

In the frame of a collaboration between ENEA and a Polish Research Institute in Warsaw, the IChTJ (Institute of Nuclear Chemistry and Technology) prepared the cathodes by means of a sol–gel process [8]. The starting sol used in complex sol–gel process (CSGP) have been prepared by adding LiOH to aqueous acetates solution of  $\text{Co}^{2+}$  with ascorbic acid, then alkalizing with aqueous ammonia to pH 8. In these sols, diluted with ethanol, porous cathodes plates have been dipped and withdrawn at controlled rate several times to achieve the required film thickness. The coated substrate was soaked at  $200^\circ\text{C}$  for 72 h, then at  $400^\circ\text{C}$  for 1 h and calcined (using low heating and cooling rate  $1^\circ\text{C min}^{-1}$ ) at  $650^\circ\text{C}$  up to 4 h. During heat treatments nickel plates were always placed between ceramic sheets to avoid waving.

### 2.2. Cathode characterization

Thermal treatment procedure has been elaborated on the basis of thermal analysis data (TGA/DSC, TA Instruments). To confirm the formation of  $\text{LiCoO}_2$  crystalline phase on the porous nickel surface, X-ray diffraction measurements were carried out after final thermal treatments using focused and monochromated Co  $K\alpha$  radiation (Italstructures). The morphology of the cathode coated with  $\text{LiCoO}_2$  was examined by scanning electron microscopy (JEOL JSM 5510 LV) and EDX analysis (IXRF 500). The mechanical strength of the cathodes was measured by four points bending test to analyse the effect of covering and thermal treatments. The electrical conductivity of cathodes was measured by a dc technique following the Van der Pauw method [9] in the temperature range of  $500\text{--}850^\circ\text{C}$ , as a function of time.

### 2.3. Cell tests

The nickel cathode coated with a layer of  $\text{LiCoO}_2$  doped with Mg, was tested in a molten carbonate fuel cell with  $10\text{ cm} \times 10\text{ cm}$  electrode area. The cell was assembled with a Ni–5 wt.% Cr anode, a  $\gamma\text{-LiAlO}_2$  matrix and a Li/K carbonate electrolyte (molar ratio 62:38). The cell performance was studied at  $650^\circ\text{C}$  and 1 atm for more than 1000 h. The cath-

ode kinetic was investigated by changing the partial pressure of oxygen and carbon dioxide. Polarization curves were obtained by an electronic load (N3300 Agilent). Current interruption is the technique used for correcting measured cell voltage for the ohmic potential drops. The initial fast change of the cell voltage when current is applied or interrupted, is recorded by an NI acquisition card with an acquisition rate of  $2000\text{ samples s}^{-1}$ . A LabView software, compiled for this purpose, controls the acquisition card.

## 3. Results and discussion

### 3.1. Characterization of the cathode coated with $\text{LiMg}_{0.05}\text{Co}_{0.95}\text{O}_2$

Fig. 1 shows the XRD patterns of the electrode after the thermal treatments: the  $\text{LiCoO}_2$  phase was observed suggesting that at  $650^\circ\text{C}$ , the formation of a layer of lithium cobaltite on the porous nickel electrode has taken place [10]. In Fig. 2 are shown the porous nickel electrode covered with a layer of magnesium doped lithium cobaltite (a), a SEM image ( $35\times$ ) of the sample situated at 2 cm from the edge of the electrode (b), a SEM image of the same sample at higher magnifications (c). Lithium cobaltite particles homogeneously cover the nickel substrate. In spite of the relatively variable concentration of cobalt on the electrode surface (Fig. 3) the layer of lithium cobaltite seems to be thin and uniform.

Four points bending tests were carried out on the electrode. Samples were taken in different positions and analysed. The average strength value  $\sigma_m = 2.59 (\pm 0.21)\text{ kgf mm}^{-2}$  is very close to literature values for similar materials [11].

Conductivity measurements were carried out on three different electrodes [12,13]:

- a conventional porous nickel sheet partially oxidized;
- a Mg-doped lithium cobaltite made in ENEA laboratories;
- a porous nickel electrode coated with Mg-doped lithium cobaltite.

To compare the electrical conductivity of materials with different porosity [14], the measured conductivity was converted

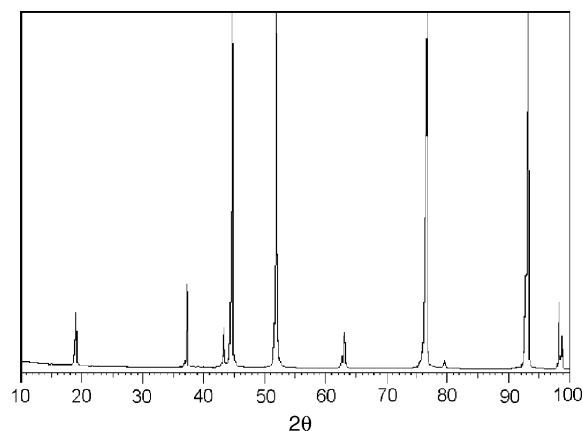


Fig. 1. XRD pattern of the  $\text{LiMg}_{0.05}\text{Co}_{0.95}\text{O}_2$  coated Ni porous electrode.

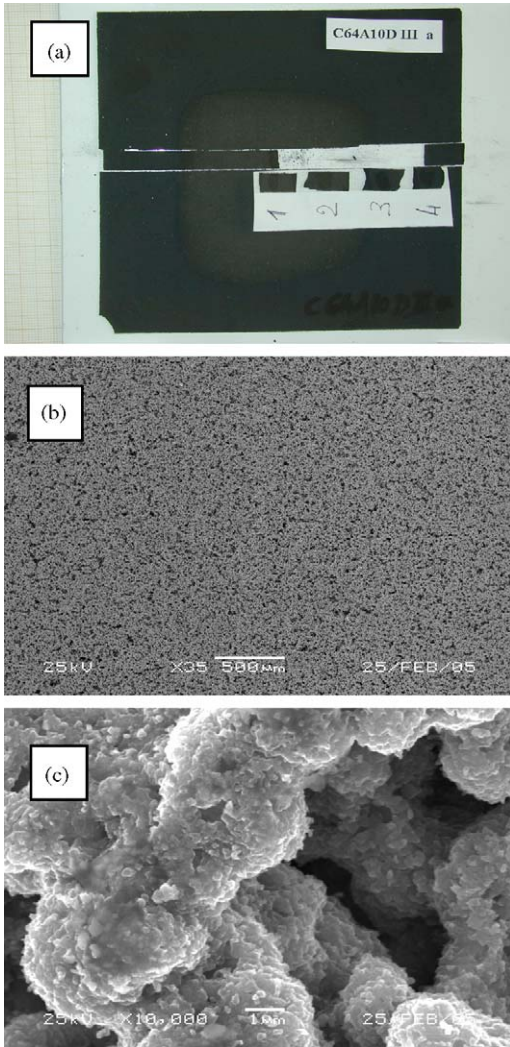


Fig. 2. (a) Lithium cobaltite/Ni electrode, (b) SEM image (35×) of the sample situated at 2 cm from the edge of the electrode and (c) SEM image (10,000×).

to the specific conductivity (conductivity at theoretical density) using the semi empirical relationship  $\sigma_0 = \sigma(1 - P)^{-1.75}$  where  $\sigma$  is the measured electrical conductivity,  $\sigma_0$  is the specific electrical conductivity and  $P$  is the porosity fraction. In Fig. 4(a) is shown the electrical resistance as a function of time in air of nickel oxide, nickel covered by lithium cobaltite and lithium cobaltite. Nickel oxide shows a resistance of 85  $\Omega$ , higher than that of lithium cobaltite (40  $\Omega$ ) and nickel coated

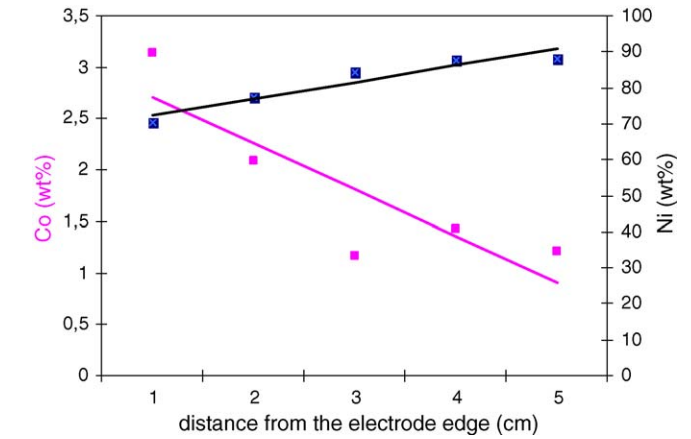
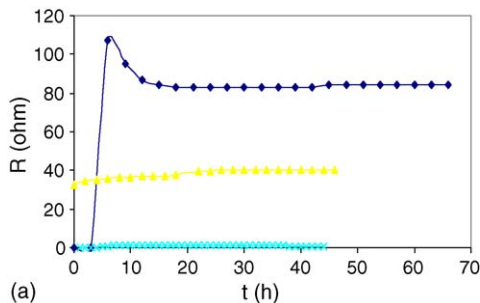


Fig. 3. Nickel and cobalt concentration profiles obtained by EDS analysis.

with lithium cobaltite (1  $\Omega$ ). The reason for the nickel oxide behaviour is the absence of lithium ions intercalation, which induces strong p-type semiconductor properties in the compound and increases conductivity significantly. Arrhenius plots for the electrical conductivity in air of nickel oxide, nickel covered by lithium cobaltite and lithium cobaltite are described in Fig. 4(b). From these plots the activation energy for the conduction process was calculated for nickel oxide and nickel covered with lithium cobaltite. The obtained values are very close: 0.21 eV for NiO and 0.22 eV for the covered electrode.

### 3.2. Cell performance

The Ni/lithium cobaltite cathode was tested in a 100 cm<sup>2</sup> electrodes fuel cell with conventional anode and tile. The cell operated for about 1000 h at 650 °C. The Fig. 5 shows the open circuit voltage (OCV) and the cell voltage at different currents and different cell lifetimes. Data are concerning with the gas composition 10/10/1 NI h<sup>-1</sup> of H<sub>2</sub>/N<sub>2</sub>/CO<sub>2</sub> and 7/0/16 NI h<sup>-1</sup> of O<sub>2</sub>/N<sub>2</sub>/CO<sub>2</sub>. The cell voltage at high current densities remained constant up to the end of the test. In Fig. 6 polarizations curves at the same gas composition but at different cell lifetime are shown. The cell performance gradually improved during the cell operation time, showing a voltage of 800 mV at a current density of 100 mA cm<sup>-2</sup> after 700 h; the carbonate electrolyte which initially filled the cathode pores is redistributed in the first hours reducing cathode polarization.

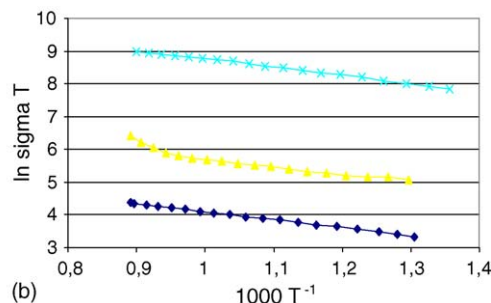


Fig. 4. (a) Electrical resistance at 650 °C as a function of time in air of nickel oxide (◆), nickel covered with lithium cobaltite (X) and lithium cobaltite (▲). (b) Arrhenius plot for the electrical conductivity in air of nickel oxide (◆), nickel covered by lithium cobaltite (X) and lithium cobaltite (▲).

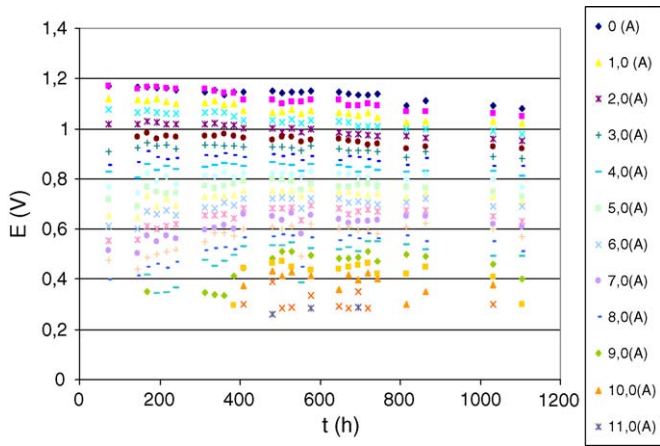


Fig. 5. Open circuit voltage (OCV) and cell voltage at different current densities at different cell lifetimes.

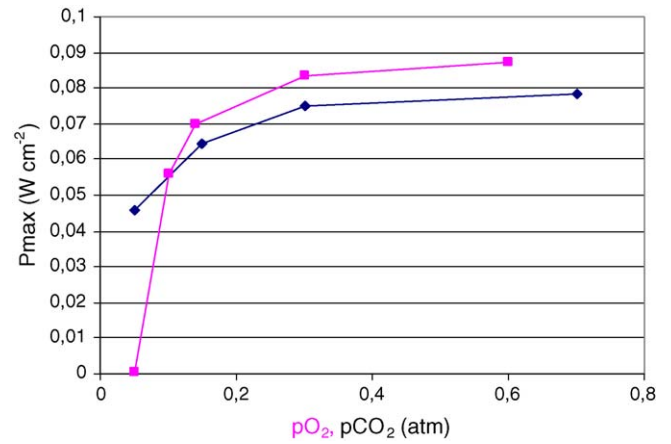


Fig. 7. Dependence of cell power from  $p_{O_2}$  and  $p_{CO_2}$ .

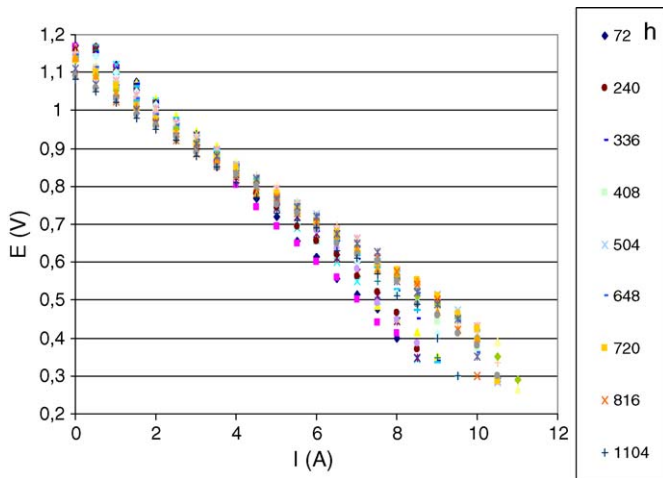


Fig. 6. Polarization curves at the same gas composition but at different cell lifetime.

The cathode kinetic was investigated by changing the oxygen and carbon dioxide partial pressures. Data of Fig. 7 refer to 648 h of cell life, and confirm the marked dependence of power from  $p_{O_2}$ , especially at low partial pressure. On the contrary, the influence of  $p_{CO_2}$  is lower for all partial pressures. The electrochemical performance of the cell increased as the oxygen and carbon dioxide partial pressure are increased indicating a positive effect on the cathode kinetic.

Table 1

The ohmic potential drop ( $IR$ ) of the cell measured by the current interruption technique at different applied currents and cell lifetime

$I$ (A)	$R$ ( $\Omega \text{ cm}^2$ )		
	72 h	360 h	744 h
0.50	4.029	3.555	4.029
1	4.029	3.614	3.851
2	3.555	3.732	3.436
Average	3.871	3.634	3.772

The ohmic potential drop ( $IR$ ) of the cell was measured by the current interruption technique. Measurements were made with different applied current at different cell lifetime described in Table 1. No differences in  $IR$  values ( $\sim 4 \Omega \text{ cm}^2$ ) [15] were evidenced that means the material was stable after the thermal treatments, which were made at the end of the sol–gel process.

### 3.3. Post-test analysis

In Fig. 8 are shown SEM pictures of the electrode before (a) and after (b) in cell test (about 1000 h cell lifetime). Some changes in morphology and grain size occurred on the electrode surface: the large open porosity decreased and the electrode skeleton was constituted by bigger grains and smaller one, which had the same chemical composition.

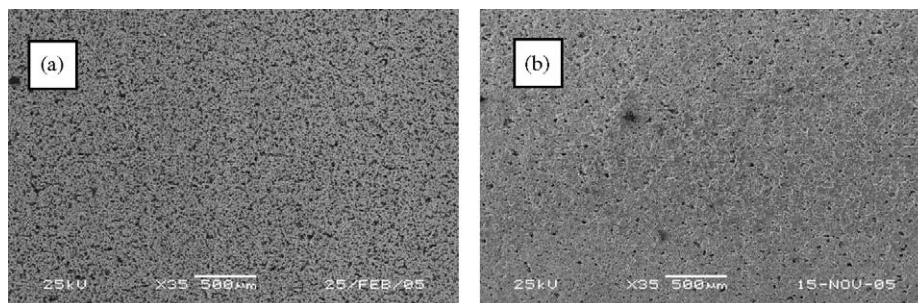


Fig. 8. SEM pictures of the electrode before (a) and after (b) in cell test (about 1000 h cell lifetime).

#### 4. Conclusions

A nickel electrode covered with a thin layer of lithium cobaltite doped with magnesium, was fabricated by complex sol–gel process (CSGP). After the covering process, the electrode was submitted to thermal treatments to allow the formation of Mg–LiCoO<sub>2</sub> layer. Chemical physical characterizations have shown the necessary requirements for a good cathode material. In cell tests showed a good cell performance that gradually improved during the cell operation time, showing a voltage of 800 mV at a current density of 100 mA cm<sup>-2</sup> after 700 h. Further investigation to improve mechanical resistance, cell performance and to streamline the electrode production are in progress.

#### References

- [1] Y. Miyazaki, M. Yanagida, S. Tanase, K. Tanimoto, T. Kojima, N. Ohtori, H. Okuyama, T. Kodama, K. Morimoto, I. Nagashima, C. Nagai, H. Itoh, Proceedings of 1992 Fuel Cell Seminar, Tucson, USA, November 29–December 2, 1992.
- [2] Y. Miyazaki, M. Yanagida, K. Tanimoto, T. Kojima, N. Ohtori, T. Asai, Proceedings of 1994 Fuel Cell Seminar, San Diego, USA, November 28–December 1, 1994.
- [3] A. Lundblad, Doctoral Thesis, Stockholm, 1996.
- [4] L. Giorgi, M. Carewska, S. Scaccia, E. Simonetti, F. Zarzana, *Denki Kagaku* 6 (1996) 482.
- [5] L. Giorgi, M. Carewska, E. Simonetti, S. Scaccia, F. Croce, A. Pozio, in: C.A.C. Sequeira, G.S. Picard (Eds.), *Electrochemical Technology of Molten Salts*, Trans Tech Publications, Switzerland, 1993, pp. 285–302.
- [6] T. Fukui, H. Okawa, K. Koderu, T. Tsunooka, Proceedings of the 2nd International Fuel Cell Conference, Kobe, Japan, February 5–8, 1996.
- [7] G.L. Lee, J.R. Selman, L. Plomp, *J. Electrochem. Soc.* 140 (1993) 390.
- [8] A. Deptula, W. Lada, *J. New Mater. Electrochem. Syst.* 6 (2003) 33–37.
- [9] J. Van der Pauw, *Philips Res. Rep.* 13 (1958) 1–9.
- [10] A. Deptula, W. Lada, Research contract ENEA-ICH TJ, 1998.
- [11] B.H. Ryu, I.G. Jang, K.H. Moon, J. Han, T.-H. Lim, TCP Paper no. 051202, 2005.
- [12] M. Carewska, F. Pallini, S. Scaccia, RTI/ERG/TEA/96(02).
- [13] L. Giorgi, M. Carewska, M. Patriarca, S. Scaccia, E. Simonetti, A. Di Bartolomeo, *J. Power Sources* 49 (1994) 227–243.
- [14] A. Wijayasinghe, B. Bergman, C. Lagergren, *J. Electrochem. Soc.* 150 (5) (2003) A558–A564.
- [15] S.G. Kim, S.P. Yoon, J. Han, S.W. Nam, *J. Power Sources* 112 (2002) 109–115.